Research Article | DOI:10.5281/zenodo.18056290
www.jnanosam.com

NANOSAM
Journal of NanoScience in Advanced Materials

Superconductivity Properties of Bi-2223 Ceramics Substituted with Strontium Sites at Large Scale Nano-Sized Europium Nanoparticles

Mehmet Ersin Aytekin[1#]

Ceramic superconductor materials with an initial composition of $Bi_{1.7}Pb_{0.3}Sr_2Ca_2Cu_{2.75}Na_{0.25}O_y$ and doping ratios of x = 0, 0.2, 0.25 and 0.3 were produced using the solid-state reaction method The effect of substituting high-nano-sized europium (80 nm) for Strontium on phase formation, morphological structure and superconducting properties were analysed using X-ray diffraction (XRD), scanning electron microscopy (SEM), electrical resistivity (R-T) and magnetisation (M-H) measurements. XRD measurements revealed the formation of the Bi-2223 high-temperature phase, the Bi-2212 low-temperature superconducting phase, and secondary phases in all samples. Despite the formation of secondary phases, the primary phase structure was superconducting in all samples. However, the phase structure gradually deteriorated with increasing amounts of nanoparticle substitution. Scanning electron microscopy (SEM) microstructure analysis of the samples showed the existence of plate-like grains, which suggested the production of both B-2212 and Bi-2223 grain structures. In the electrical measurement results, superconductivity was exhibited in the samples up to the substitution value x = 30. In the sample containing nano-sized Eu at x = 0.20, the value of the superconductivity transition temperature increased due to the decrease in impurity phase density. M-H measurements were performed to characterize the magnetic properties of the samples. In M-H measurements, closed-loop hysteresis, a characteristic feature of Bi-2223 superconductors, occurred in a uniformly shaped sample containing no nano-sized europium. However, the hysteresis area decreased with increasing substitution, indicating a deterioration in magnetic properties.

1. Introduction

Due to their unique properties, such as high superconductivity, critical transition temperatures (Tc), magnetic field carrying capacities (Hc) and critical current density (Jc), high transition temperature superconductors are targeted for use in advanced engineering applications, such as power transmission cables, medical diagnostics and heavy industry technology [1,2].

Among the families of copper-oxide superconductors, the bismuth-based high-temperature superconductors have the advantages of high thermodynamic stability, an absence of harmful precursors, an easy synthesis process and a transition temperature above the temperature of liquid nitrogen [3.4]

Bismuth-based high-temperature superconductor systems with the general formula $Bi_2Sr_2Ca_{n-1}Cu_nO_{4+2n}$ have three different phases. According to the value of n, which defines the number of copper oxide layers in the unit cell in the general formula and is related to the superconducting transition temperature, the Bi-2201 phase with a transition temperature of about 20 K for n= 0, the Bi-2212 phase with a transition temperature of about 80 K for n= 1, and the Bi-2223 superconducting phases with a transition temperature of about 120 K for n= 3 are formed [5,6] High-capacity power transmission cables, high-magnetic capacity magnet applications, and high-efficiency rotor applications can all benefit

---

[1] *Tarsus University, Electronics and Automation, Vocational School of Technical Sciences at Mersin Tarsus Organized Industrial Zone, 33100, Mersin, Türkiye*

#Corresponding author:mehmetaytekin@tarsus.edu.tr

Keywords: $Bi_{1.7}Pb_{0.3}Sr_2Ca_2Cu_{2.75}Na_{0.25}O_y$; SEM; Nano-sized Europium; R-T

Received: 21 September 2025 | Accepted: 03 November 2025 | Published online: 30 December 2025

from the usage of BSCCO superconducting materials because of their specific electrical and magnetic characteristics, consistent morphological structure, and phase stability [7,8]. However, because superconducting conditions are easily achieved at liquid nitrogen temperatures, BSCCO researchers aimed to reach higher temperatures at *Jc* values by modifying the morphological structures. As is known from the literature, in order to reach high Jc values, additional flux pinning centers should be created by adding various nano-oxides to the system [9,10]. Moreover, previous studies have shown that creating suitable crystal defects inside the BSCCO superconducting matrix that can serve as pinning centres is an effective method of increasing the current-carrying capacity in the presence of an applied magnetic field [11]. In particular, studies on the addition/doping of nanosized materials to the BSCCO crystal structure have shown that, compared to micro-scale chemicals, nanoparticles form stronger bonds between superconducting grains and improve flux pinning properties. Furthermore, the presence of nano-sized rare earth elements between superconducting grains may increase the possibility of increasing the number of flux pinning centers in impurity phases [12,13]. The effect of nano-sized europium particles on BSCCO superconducting systems has not yet been extensively investigated in the literature.

In our previous study, nano-sized Eu (80 nm) was substituted into the strontium oxide layer of the $Bi_{1.7}Pb_{0.3}Sr_2Ca_2Cu_{2.75}Na_{0.25}O_y$ superconducting structure at different ratios (x= 0.00, 0.025, 0.050, 0.1 and 0.15). The findings revealed that superconductivity and magnetic properties increased up to x > 0.15 [14]. In the present study, the effect of higher substituting ratios such as x = 0.2, 0.25 and 0.30 on the initial composition of $Bi_{1.7}Pb_{0.3}Sr_2Ca_2Cu_{2.75}Na_{0.25}O_y$ was investigated. The effects of high concentrations of europium nanoparticles on phase formation, microstructures, electrical and magnetic properties of ceramic superconductor samples produced by the classical solid state reaction method were investigated using X-ray diffraction, scanning electron microscopy, resistivity and magnetization measurements, respectively.

2. Results and Discussion

Figure 1 shows the pattern obtained from the XRD measurement results of the samples. In the X-ray diffraction measurement results, the Bi-2223 (JCPDS NO: 00-042-0450) superconductivity phase is symbolized by +, while the Bi-2212 (JCPDS NO: 98-006-7428) superconductivity phase, $Ca_4Bi_6O_{13}$ (JCPDS NO: 00-048-0217) phase, $Ca_{0.2}Sr_{1.8}PbO_4$ (JCPDS NO: 00-048-1516) phase, Bi_2CaO_4 (JCPDS NO: 01-082-1982) phase and $CaPbO_3$ (JCPDS NO: 00-051-1704) " are symbolized by ●, ■, ⋆ and ▲.

X-ray diffraction analyses show that the main phase structure in all samples is the Bi-2223 phase. However, with the introduction of large scale of nano-sized Eu substituting into the system, a decrease in the intensity and density of the Bi-2223 phase occurred.

In ceramic superconducting materials, a low impurity phase content and high-intensity characteristic peaks may indicate the formation of a good crystallization process [15]. Furthermore, the presence of nanoparticles within the superconductor system and the formation of certain impurity phases can enhance *Jc* performance by improving flux pinning mechanisms [16]. Minor impurity phases that act as flux pinning centers and the successful formation of crystallization processes significantly affect superconducting performance.

In the B sample containing nano-sized europium at x = 0.20, $CaPbO_3$ impurity phase formation was observed at points such as 2θ ≈ 29.30° and 32.34°, while Bi-2212 low-temperature superconductivity phase was observed at points such as 2θ ≈ 37.74°, 49.72° and 59.38°. Erdem et al. reported developments in the phase structure and an increase in the superconducting transition temperature in the Bi-2212 superconducting system doped with Ho^{3+} [17]. Furthermore, Sample B showed an increase in the intensities of the peaks associated with the Bi-2223 high-temperature superconducting phase, which may have improved the superconductivity characteristics. No significant differences are evident when Sample C, which contains nano-sized europium at x = 0.25, is compared with Sample B. On the other hand, in sample D containing x = 0.30 europium, the low-temperature phase that occurred as Bi-2212 phase in the previous samples transformed into $Ca_4Bi_6O_{13}$ impurity phase. Additionally, the intensity of the distinctive Bi-2223 phase peaks decreased. Yakıncı et al. reported that the superconducting properties of the nickel-doped Bi-2212 system deteriorated as a result of a decrease in the density of the high-temperature superconducting phase and the peak intensity with increasing doping [18].

The average size of a crystal is determined by the Debye-Scherrer equation as follows [19]:

$$\frac{\kappa\lambda}{\beta cos\theta} \qquad (1)$$

where λ is the x-ray wavelength (CuKa=1.5406 Å), κ is the crystallite shape factor (0.94), β is the peak full width at half maximum at the observed peak angle θ (in radians).

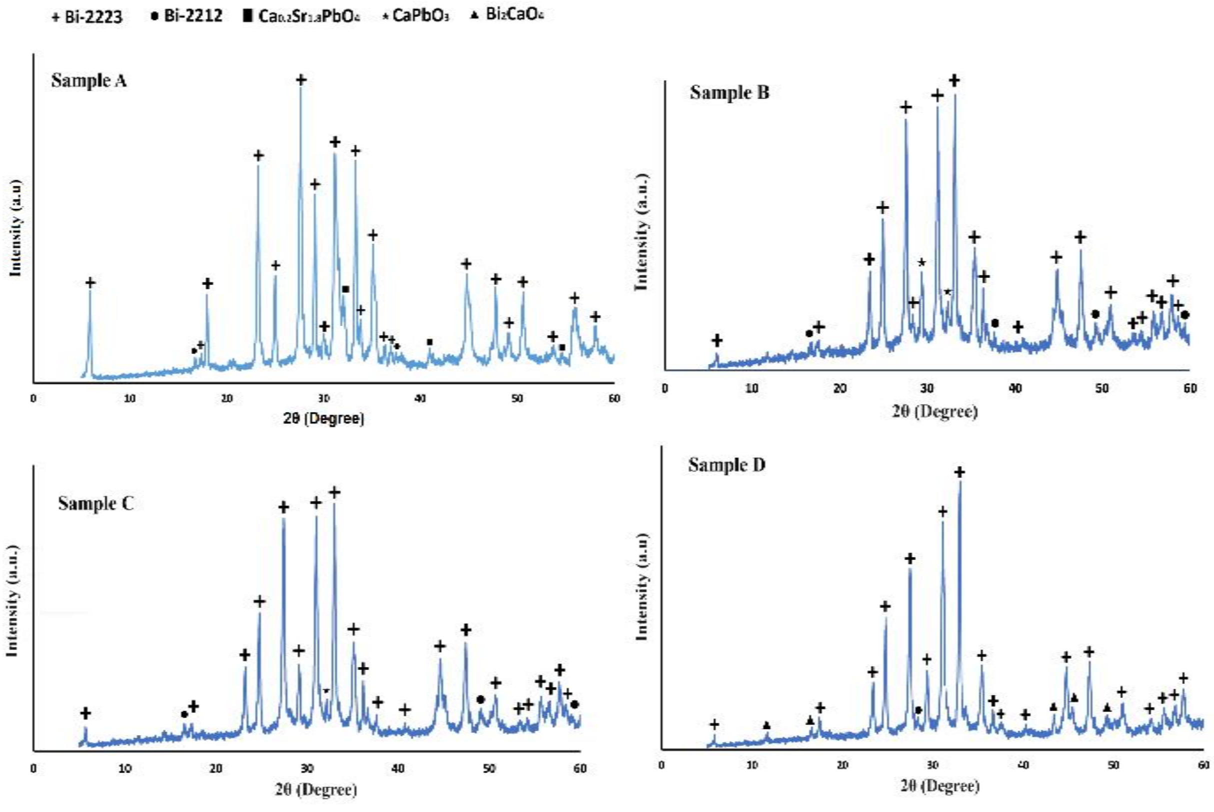

Figure 1. X-ray diffraction pattern of samples containing high nano-sized europium substituting.

The crystal average size values of the samples are given in Table 1. The Debye-Scherrer equation was used to calculate the crystal size values for samples A, B, C and D, which were found to be approximately 32.116, 23.457, 24.897 and 25.913 nm, respectively. In order to achieve high *Jc* values, good connections between superconductor grains are required. The substitution of nano-sized elements to the system can create a good crystallisation effect by improving the bonds between the grains. A decrease in the average crystal value was observed with the increase of europium substituting at nanosized in the samples.

The samples exhibit tetragonal symmetry, as seen in Table 1. The lattice parameter values are in agreement with those of the Bi-2223 phase with tetragonal symmetry as reported in the literature [6,20]. The substitution of europium at different quantities resulted in different values of the lattice parameter in the samples. Changes in repulsive forces were observed at different concentrations, which was consistent with changes in the oxygen concentration within the BSCCO sandwich structure. As is well known, changes in the lattice parameter c can be related to the superconductivity transition temperatures of the samples. When we look at the c lattice parameter value in Table 1, the value closest to the optimum process was obtained in the sample containing nano-sized europium at x = 0.20.

The following expressions were used to calculate the phase percentages of Bi-2223 and Bi-2212 [21].

$$\text{Bi-2223 (\%)} = \frac{\Sigma I2223}{\Sigma I2223+\Sigma I2212} \text{ x } 100\%$$

$$\text{Bi-2212 (\%)} = \frac{\Sigma I2212}{\Sigma I2223+\Sigma I2212} \text{ x } 100\%$$

where I is the percentage of volume of the phases. Volume fraction of Bi-2223 and Bi-2212 and impurity in ceramic samples with different amounts of nano-sized Eu substituted phases are shown in Table 1.

Table 1. Lattice parameter values of ceramic superconductor samples.

Sample	**a (Å)**	**b (Å)**	**c (Å)**	**Grain Size (nm)**
Sample A	5.369	5.369	36.943	32.116
Sample B	5.396	5.396	37,632	23.457
Sample C	5.401	5.401	37.545	24.897
Sample D	5.407	5.407	36.892	25.913

Table 2. Crystal phase distributions of ceramic samples

Samples	Bi-2223 (%)	Bi-2212 (%)	Impurity Phase (%)
Sample A	84.94	0.61	14.43
Sample B	86.235	9.782	3.981
Sample C	74.468	3.768	21.762
Sample D	74.098	11.255	14.645

Changes in the phase distributions of the samples by substituting nano-sized europium can be seen in Table 1. It can be seen that the volume percentage of Bi-2223 phase has improved in Sample B. Compared to the sample without nano-sized Europium, the substitution of europium nanoparticles at x = 0.20 contributes to the development of the Bi-2223 phase. It is found that the sample at higher substitution rates shows a reduction in the volume of the Bi-2223 phase.

To perform surface analysis of the samples, scanning electron microscope (SEM) measurements were performed at 15 K magnification. SEM measurement results are shown in Figure 2.

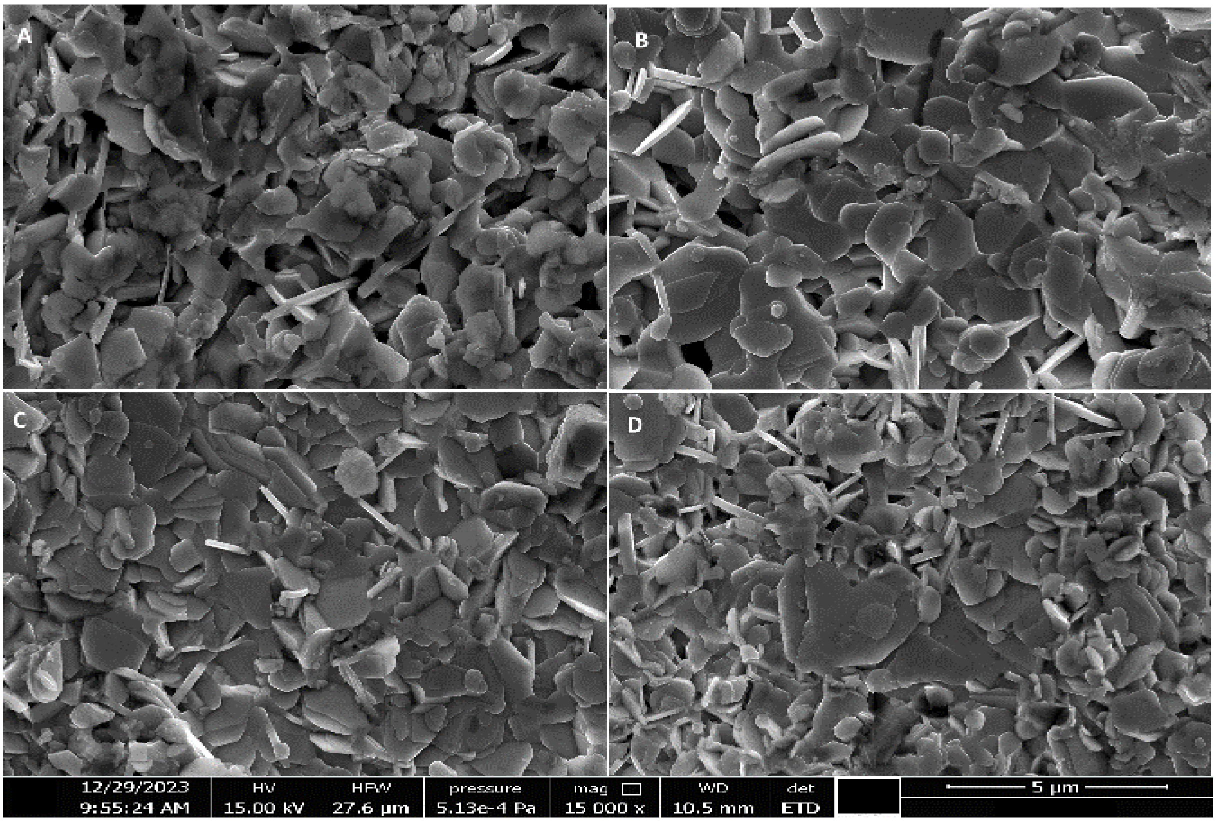

Figure 2. Microstructure results of Bi,Pb-2223 superconductor samples with high content of europium nanoparticles substituting.

In ceramic superconducting samples, intergranular porous structures naturally occur. As is well known, the reduction of porous structures between superconducting grains and the formation of strongly bonded grains improve superconductivity parameters [23, 24]. Many research groups have aimed to eliminate defects in the morphological structure to increase its use in technology. The most useful method is to adding/dopping nanoparticles of different sizes and atomic radii [24]. Suhaimi et al. reported improvements in *Jc* and magnetic properties as a result of obtaining modifications in the morphological structure of the Eu-containing sample at a nano-sized ratio of 0.025 [25]. Thus, Eu substitution at the nanoscale may be a candidate for morphological modifications in BSCCO systems.

The Bi-2223 phase is indicated by the production of flaky plate-like grains in the SEM data, whereas the existence of Bi-2212 superconducting phases is indicated by the plate-like grain structures [26,27]. In the microstructure analysis results of all samples, plate-like grain and flaky grain formations were observed in both structures, indicating the co-formation of Bi-2223 and Bi-2212 superconducting phases, in agreement with the X-ray diffraction results. Larger grains, fewer grain borders, and strongly connected grain structures are necessary for the morphological structure of superconductors in ceramic materials to show greater current-carrying capabilities. Therefore, significant modifications to the microstructural properties of ceramic superconductors are necessary in order to use them in areas where high technology is needed.

Examining the microstructural properties of the samples in Figure 2 reveals the formation of randomly oriented grains separated by grain boundaries, which is characteristic of samples produced by the solid-state reaction method. In addition, as the substitution ratio changed, some modifications occurred in the surface structure of the samples. In sample B, europium nanoparticles at x = 0.20 supported the formation of large-sized plate-like grain and less porous structures. In addition, at higher additive rates, grain sizes decreased and grain boundaries increased.

Figure 3 shows the results of the resistivity temperature measurements performed to determine the superconductivity transition temperatures of the samples. While the R-T results of all examples are shown in Figure 3(a), a detailed representation of Sample A is given in (b).

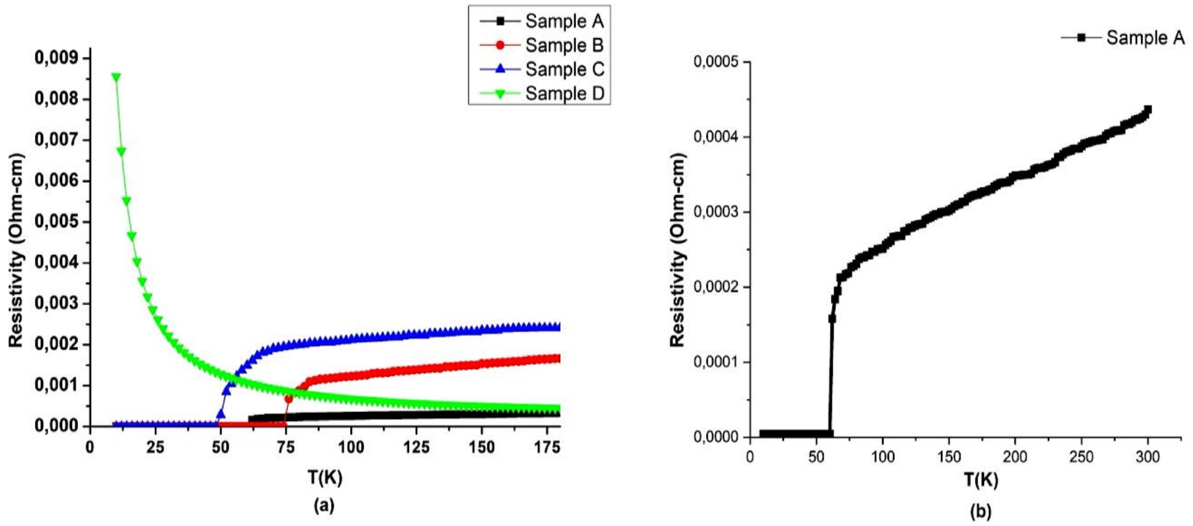

Figure 3. Resistivity-temperature graph of samples.

Copper-oxide superconducting ceramics are systems that are highly consistent with the BSC theory, which successfully explains superconductivity [28]. The BCS theory explains electron pairing mechanisms, known as Cooper pairs, with the assistance of phonons. Within the system, the formation of electron pairs only occurs below a certain temperature (the superconducting transition temperature, *Tc*) [29]. The smooth pairing of electrons within the system, the minimal presence of factors that disrupt electron pairs (such as inhomogeneous conditions, impurity phases, and externally applied high magnetic fields), and the strong interaction between pairs determine the superconducting properties [30].

In Bi-based superconductor systems with high transition temperatures, the T_c^{onset} temperature value, which is the first transition to the superconducting phase in materials, depends on the ratio of superconducting phases in the crystal structure, while the T_c^{offset} temperature value, where the superconducting transition is completed, is related to the connections between the phases formed in the crystal structure [31,32]. When metallic elements enter the BSCCO superconductor system, cation and anion structures can easily enter the crystal structure and alter parameters such as the angle and orientation of the grains and the number of defects, as well as the amount of oxygen. Moreover, these elements substituted into the system can contribute to obtaining optimum hole concentration in the system by transferring extra charge to the charge carriers of the BSCCO system when they enter the crystal structure. Thus, achieving such improvements in BSCCO ceramic superconductors increases the transition temperature of the system. Obtaining the optimum carrier concentration by introducing elements with different ionic radii into the superconductor can increase the superconductivity transition temperatures by contributing to the development of the superconducting phase formation and the strengthening of the inter-grain connections in the morphological structure.

The transition temperature values of the samples are shown in Table 3. The SEM measurement results for sample A revealed an irregular distribution of grains within the void structure. Such detrimental impacts on the morphological structure might be evidence of poor homogenous structure and crystal defects, which could also have an impact on the value of the superconducting transition temperature. In Sample B, a slight increase in the transition temperature values occurred because the 0.20 nano-sized Eu particles modified the superconductivity properties. In sample C, the transition temperature value decreased because the high content of europium nanoparticles (x = 0.25) caused the intensity and volume of the Bi-2223 superconductivity phases to decrease. In sample D, superconducting transition did not occur due to negative effects such as impurity phases weakening the connections between superconducting phases and damaging the carrier charges. The improvement in the superconductivity transition temperature values in the sample containing nano-sized Eu at x = 0.20 also indicates that the Cooper pair formation is supported in this sample. Furthermore, superconductivity is not observed in sample D due to the large quantity of nano-sized Eu doping, which prevents the formation of Cooper pairs.

In ceramic superconductor materials, the onset and offset temperature difference is called ΔTc and is related to the homogeneous phase structure within the material [33]. Additionally, for good superconductivity performance, the transition from onset temperature to offset temperature must be sharp [34]. Kocabaş et al reported that the ΔTc value decreased due to the development of a homogeneous structure and the formation of strong bonds between grains as a result of the addition of 0.10% MgO to the copper oxide sites in Bi-2223 superconductors [35]. In the X-ray phase analysis of the sample containing Eu nanoparticles at a ratio of x = 0.20, there was an increase in the density of the Bi-2223 phase and a decrease in the proportion of the impurity phase. As a result of these developments, a decrease in the ΔTc value occurred in sample B.

In order to characterize the magnetic properties of ceramic samples containing different amounts of nano-sized europium, M-H measurements were carried out at 15 K and 25 K temperatures under a magnetic field of ± 20000 Oe. M-H measurements of samples A, B and C performed at two different temperatures are detailed in another study [36]. The M-H results of sample D, performed at 15 K and 25 K temperatures under a magnetic field of ± 20000 Oe, are shown in Figures 4 and 5.

The width and geometry of the hysteresis field in M-H plots are affected by the quality of inter-grain connections, grain orientations and homogeneity in ceramic superconducting materials [37,38].

Table 3. The transition temperature value of the superconducting samples.

Samples	T_c^{onset} (K)	T_c^{ofset} (K)	ΔT_c (K)
Sample A	80.073	60.116	19.957
Sample B	90.089	74.084	16.005
Sample C	70.106	48.145	21.961
Sample D	Sample D is not a superconductor.		

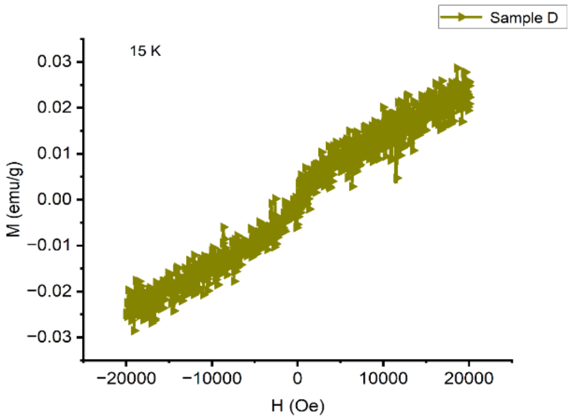

Figure 4. M-H results of Sample D under 15 K temperature and ± 20000 Oe magnetic field

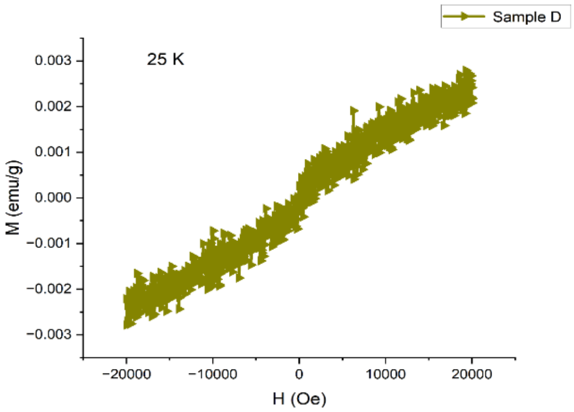

Figure 5. M-H results of Sample D under 25 K temperature and ± 20000 Oe magnetic field

Additionally, the M-H performance might be affected by the homogenous crystal structure development and the quality of the superconducting phases. In the M-H measurements carried out at both temperatures for the A Sample, which does not contain Eu at the nano-sized, the area covered by the hysteresis graph and its geometry generally exhibit the characteristic behavior of BSCCO superconductors [36]. With the increase of europium substituting at nano-sized, the volume of superconducting phases decreased, causing irregularities and decreased homogeneity in the microstructure. In addition, a higher nano-sized europium substitute has weakened magnetic performance by causing the formation of impurity phases and weakening Cooper pair mechanism. The hysteresis field decreased as a result of this behavior in the samples, and the geometry was deformed to a contribution ratio of x <0.30. Furthermore, since europium nanoparticles in the nano size range up to x < 0.30 cannot act as flux pins, they do not contribute to magnetic performance. At x = 0.30 substitution rate, the hysteresis behavior is deteriorated.

3. Conclusion

In the current study, nano-sized europium (x = 0.0, 0.2, 0.25 and 0.30) was substituted into the $Bi_{1.7}Pb_{0.3}Sr_2Ca_2Cu_{2.75}Na_{0.25}O_y$ system at different rates (large-scale). The samples produced by the solid state reaction method were characterized by X-ray powder diffraction, scanning electron microscopy, resistivity-temperature and M-H measurements. In the X-ray measurement results, despite the formation of secondary phases and low-temperature Bi-2212 phase in all samples, the main phase structure is Bi-2223 phase. Some modifications occurred in the formation of the Bi-2223 phase in the sample containing nano-sized Europium at x = 0.20. In the microstructure results, the formation of flaky plate-grains and plate-like grain structures were detected, indicating the co-formation of Bi-2223 and Bi-2212 phase structures. In resistivity-temperature measurements, superconductivity transition was obtained in samples up to $x < 0.30$ substituting ratio. Non-superconducting behavior was observed in the sample with the substitution value x = 0.30. In M-H measurements performed to characterize magnetic properties, hysteresis properties with a regular structure were observed in the sample without europium at the nano-sized. The increase in substitution value caused a deterioration in magnetic properties.

In the findings obtained, despite exhibiting weak characteristics in terms of M-H performance, the best superconductivity transition temperature value of 90.09 K was obtained in the sample containing europium at a ratio of x = 0.20 in nano size, which is a promising result as a superconducting cable.

Method

Polycrystalline $Bi_{1.7}Pb_{0.3}Sr_{2-x}(Eu)_xCa_2Cu_{2.75}Na_{0.25}O_y$ (x= = 0, 0.2, 0.25 and 0.3) ceramic samples were produced by the standard solid state reaction method using high purity precursor powders of Bi_2O_3 (Thermo, 99%), PbO (Tekkim, 99%), $SrCO_3$ (Thermo, 99%), $CaCO_3$ (Thermo, 99%), CuO (Thermo, 99%), $NaCO_3$ (Thermo, 99%) and Eu_2O_3 (80 nm) (Nanografi, 98.5+%). Firstly, the precursor powders were weighed in proportions appropriate to stoichiometric calculations. Then, the precursor powders were ground in an agate mortar to obtain a homogeneous mixture. After grinding, the homogeneous powder mixtures were pressed under 375 MPa pressure to form pellets with a diameter of 1.3 cm. After that, the pellets were subjected to a 12 h calcination at 750 °C as the first heat treatment. The calcined pellets were re-ground, re-pressed and re-calcined at 820 °C for 24 h. Grinding, pressing, and heat treatment procedures were performed several times to initiate the formation of high-temperature superconducting phases. Sintering is an important process to complete the formation process of desired phases in high-temperature superconducting materials. Therefore, long periods of sintering (150–170 h) at approximately 860 °C are required for optimum formation of high-temperature Tc phases. Finally, the precursor pellets were milled, pressed and annealed at 860 °C for 170 h. The samples produced in $Bi_{1.7}Pb_{0.3}Sr_{2-x}(Eu)_xCa_2Cu_{2.75}Na_{0.25}O_y$ with x = 0.0, 0.2, 0.25 and 0.30 substituting values at initial conditions were named as Sample A, Sample B, Sample C and Sample D respectively in order to name the characterisation processes.

Resistivity and diamagnetic studies were carried out on the samples using a Physical Property Measurement System (PPMS) (5 to 150 K) capable of reaching cryogenic temperatures of about 2 K in a closed-circuit helium system. To determine the phases formed in the samples, X-ray powder diffraction analyses were performed using a Rigaku MiniFlex X-Ray Diffractometer with a constant scanning speed (2°/min) in the range of $2\theta = 3–60°$. PDXL software version 1.6.0.1 using the ICDD version 6.0 database automatically calculated the lattice parameters. The granular structure of the ceramic samples was examined using a Quanta 650 Field Emission (SEM).

Acknowledgements

The presented study was funded by TÜBİTAK with the 2218 Domestic Postdoctoral project. The author would like to thank Prof. Dr. Mustafa AKYOL, who served as a Advisor on the project, for his meticulous support. All samples were prepared in the NanoMaterials/Magnetic Materials Research laboratory (NM_3RLab) Adana Alparslan Türkeş Science and Technology University in Türkiye. SEM, XRD, M-H and R-T measurements were carried out in Çukurova University ÇÜMERLAB central laboratories in Türkiye. This work was presented as a paper at the 12th International Conference on Materials Science and Nanotechnology for Next Generation (MSNG2025). The extended full-text version has been shared in the journal. Also, the financial support for participation MSNG congress was provided by TUBITAK 2224-B Programme for Supporting Participation in Domestic Scientific Activities.

Authors' Contributions

The author participated in every step of the manuscript's development.

Data Availability Statement

The data that support the findings of this study are available from the corresponding author upon reasonable request.

Declaration of Ethical Standards

The author(s) of this article declare that the materials and methods used in this study do not require ethical committee permission and/or legal-special permission.

Funding Information

This study is supported by TUBITAK with project number 122C061 within the scope of "2218 - National Postdoctoral Research Fellowship Program".

References

[1] Yin, S., Arbelaez, D., Swanson, J., Shen, T., Epoxy resins for vacuum impregnating superconducting magnets: A review and tests of key properties, IEEE Transactions on Applied Superconductivity, **29**, 1-5, (2019).

[2] Karaçora, F., Gürsul, M., Özçelik, B., Refinement of the Bi-2212 characteristics through sodium–lithium co-doping, Journal of Materials Science: Materials in Electronics, **36**, 3-16, (2025).

[3] Al Azzawi, A.N.S.,Türköz, M.B., Erdem, Ü., Yildirim, G., Improvement in organization of Cu–O coordination and super-electrons in Bi-2212 ceramic matrix with Ag/Sr partial substitution, Journal of Materials Science: Materials in Electronics, **35**, 1261, (2024).

[4] Aytekin, M.E., Change in Physical, Electrical and Magnetic Properties of Bi-2212 Superconducting Materials Co-Substituted with Nano-Sized Zinc and Sodium, Transactions on Electrical and Electronic Materials, **25**, 779–791, (2024).

[5] Abdelhaleem, S., Noun, M.,Yousif, N.M., Shalaby, M.S., Impact of carbon nanotubes on superconducting properties and ferromagnetism of indium-doped Bi-2212 superconductors: Critical current density enhancement, Physica B: Condensed Matter, **697**, 416704, (2025).

[6] Ilhamsyah, A. Zabidi, N.A.M., Hashidi, M.A.H. , Suib, N.R.M., Mahat, A., Abd-Shukor, R., Masnita, M., Effect of copper (II) sulfide addition on the transport critical current density and AC susceptibility of $Bi_{1.6}Pb_{0.4}Sr_2Ca_2Cu_3O_{10}$ superconductor, Applied Physics A, **130**, 2-12, (2024).

[7] Frank, M., Frauenhofer, J., Van Hasselt, P., Nick, W., Neumueller, H.W., Nerowski, G., Long-term operational experience with first Siemens 400 kW HTS machine in diverse configurations, IEEE Transactions on applied superconductivity, **13**, 2120-2123, (2003).

[8] Hao, Q., Xu, X., Jiao, G., Yao, K., Liu, G., Li, C., Impact of hot isostatic pressing on the microstructure and current-carrying capacity of Bi-2212 wires, Journal of Materials Science: Materials in Electronics, **35**, 746, (2024).

[9] Shahbazi, M., Hao, Y., Patel, D., Liang, H., Yamauchi, Y.,Hossain, M.S.A., Biomass-derived carbon doping to enhance the current carrying capacity and flux pinning of an isotopic Mg11B2 superconductor, Journal of Magnesium and Alloys, **10**, 1868-1877, (2024).

[10] Verma, P.K., Reddy, B.V., Rajasekharan, Revathy, R., Varma, M.J., Seshu Bai, V., Two-Phase Microstructure Generated by Reaction of Nano WO_3 Addition and its Effect on Flux Pinning in Bi 2212 Composites. Jornal of Superconductivity and Novel Magnetism, **37**,1-4, (2024).

[11] Hernández-Wolpez, M., Gallart-Tauler, P., García-Fornaris, I., Govea-Alcaide, E., Pérez-Tijerina, E., Jardim, R.D.F., Muné, P., Trapping of Magnetic Flux in Bi-2223 Ceramic Superconductors Doped with α-Al2 O 3 Nanoparticles, Journal of Superconductivity and Novel Magnetism, **33**, 675-682, (2020).

[12] Zelati, A., Amirabadizadeh, A., Kompany, A., Salamati, H., Sonier, J., Effect of Eu_2O_3 nanoparticles addition on structural and superconducting properties of BSCCO, Journal of Superconductivity and Novel Magnetism, **27**, 1369-1379, (2014).

[13] Saghafi, M., Shams, G., Soltani, Z., The influence of Sm_2O_3 nanoparticles adding on some superconducting properties of $Bi_{1.6}Pb_{0.4}Sr_2Ca_2Cu_3O_{10+\delta}$ ceramics, Physica C: Superconductivity and its Applications, **624,** 1354566 (2024).

[14] Aytekin, M.E., Akyol, M., Modification of Magnetic and Electrical Properties of Bi, Pb-2223 Superconductors by Nano-Sized Eu Substitution, Journal of Superconductivity and Novel Magnetism, **38**, 1-15, (2025).

[15] Ozturk, O., Yildirim G., Asikuzun E., Coskunyurek M., Yilmazlar M., Kilic A., Change of formation velocity of Bi-2212 superconducting phase with annealing ambient, Journal of Superconductivity and Novel Magnetism, **24**, 4643, (2013).

[16] Shalaby, M.S., Noun, M., Yousef, N.M., Maksoud, M.A., Abdelhaleem, S., Influence of Ba substitution on phase formation, RBS analysis, critical current density and flux pinning dynamics in Y-BSCCO superconducting materials, Cryogenics, **150**, 104129, (2025).

[17] Erdem, U. Homovalent Ho/Bi substitution effect on characteristic properties of Bi-2212 superconducting ceramics, Journal of Materials Science: Materials in Electronics, **32** (24), 28587-28604, (2021).

[18] Yakinci, M.E., Madre, M.A., Ozabaci, M., Sotelo, A., Structural and superconducting properties of magnetically doped Bi-2212 textured rods grown by laser floating zone (LFZ) technique, Journal of superconductivity and novel magnetism, **26** (4), 1135-1141, (2013).

[19] Saritekin, N., Pakdil, M., Yildirim, G., Oz, M., Turgay, T., Decrement in metastability with Zr nanoparticles inserted in Bi-2223 superconducting system and working principle of hybridization mechanism, Journal of Materials Science: Materials in Electronics, **27**, 956-965, (2016).

[20] Pham, A.T., Le, T., Nguyen, H.L., Nguyen, H.N., Nguyen, T.B., Pham, P.V., Nguyen, K.M., Dang, T.B.H., Pham, N.T., Kieu, X.T., Effect of FePd nanoparticle addition on the superconductivity of Bi1.6Pb0.4Sr2Ca2Cu3O10+δ compounds, Ceramics International, **50**, 16425-16434, (2024).

[21] Cao, H., Zhang, S., Cui, Y., Wang, Y., Zhi, L., Shao, B., Liu, X., Liu, J., Li, C., Li, J. Flux pinning mechanism of Bi-2223 bulk superconductors by tuning Bi-2212 and Bi-2234 intergrowths, Ceramics International, **51**, 10014-10025, (2025).

[22] Abdelhaleem, S., Noun, M., Yousif, N.M., Shalaby, M.S., Impact of carbon nanotubes on superconducting properties and ferromagnetism of indium-doped Bi-2212 superconductors: Critical current density enhancement, Physica B: Condensed Matter, **697**, 416704, (2025).

[23] Aytekin, M.E. Modification of the electrical and magnetic properties of Bi-2212 ceramic superconductors by nano-sized europium substitution, Journal of Materials Science: Materials in Electronics, **36** (29), 1870, (2025).

[24] Abdelhaleem, S., Alziyadi, M.O., Alruwaili, A., Alawi, M.J., Alkabsh, A., Shalaby, M.S., BSCCO high Tc-superconductor materials: strategies toward critical current density enhancement and future opportunities, Applied Physics A, **131** (2), 151, (2025).

[25] Suhaimi, N.E., Hashim, A., Razali, W. A. W., Ibrahim, N., Saipuddin, S.F., Superconducting and microstructure properties of Eu2O3 nanoparticles substitution in low density Bi (Pb)-2223 superconductor, Journal of Alloys and Compounds, **1012**, 178448, (2025).

[26] Suhaimi, N.E., Hashim, A., Razali, W.A.W., Ibrahim, N., Saipuddin, S.F., Superconducting and microstructure properties of Eu_2O_3 nanoparticles substitution in low density Bi (Pb)-2223 superconductor, Journal of Alloys and Compounds, **1012**, 178448, (2025).

[27] Najem, A., Habanjar, K., Awad, R., Anas, M., Matar, M., Superconductivity investigation of (Bi, Pb)-2223 added with different nanoferrites and their composites, Physica Scripta, **99**, 095949, (2024).

[28] Bednorz J.G., Müller, K.A., Possible high Tc superconductivity in the Ba–La–Cu–O system, Zeitschrift für Physik B Condensed Matter, **64** (189), 193, (1986).

[29] Bardeen, J, Cooper, L.N., Schrieffer, J.R., Theory of Superconductivity, Physical Review, **108**, 1175–1204, (1957).

[30] Sedky, A., Ali, A.M., Somaily, H.H., Effect melting time on the excess conductivity and critical parameters of BSCCO cooper oxide system, Journal of Superconductivity and Novel Magnetism, **33** (10), 2963-2969, (2020).

[31] Awad, R., Study of the Influence of MgO Nano-Oxide Addition on the Electrical and Mechanical Properties of $(Cu_{0.25}Tl_{0.75})$-1234 Superconducting Phase, Journal of Superconductivity and Novel Magnetism, **21**, 461-466, (2008).

[32] Aytekin, M.E., Akyol, M., Özkurt, B., Improvement in electrical properties of Bi-2212 superconducting materials substituted with large-scale nano-sized tin, Applied Physics A, **130**, 78, (2024).

[33] Ozturk, O., Yildirim, G., Asikuzun, E., Coskunyurek, M., Yilmazlar, M., Kilic, A., Change of formation velocity of Bi-2212 superconducting phase with annealing ambient, Journal of Materials Science: Materials in Electronics, **24** (11), 4643-4654, (2013).

[34] Gul, I. H., Rehman, M., Maqsood, A., Temperature dependence of thermal and electrical conductivity of Bi-based high-Tc (2223) superconductor, Physica C: Superconductivity and its applications, **450** (1-2), 83-87, (2006).

[35] Kocabas, K., Özkan, O., Bilgili, O., Kadıoglu, Y., Yılmaz, H., The effects of Mg substitution in Bi-2223 superconductors. Journal of superconductivity and novel magnetism, **23** (8), 1485-1492, (2010).

[36] Aytekin, M.E., Akyol, M., Effect of Nano-Sized Europium Substitution on Strontium Sites on Diamagnetic Properties in BiPb-2223 Superconductor System, Journal of NanoScience in Advanced Materials, **3**, 8-14, (2024).

[37] Özkurt, B., Enhancement in superconducting transition temperature and Jc values in Na-doped $Bi_2Sr_2Ca_1Cu_{2-x}Na_xO_y$ superconductors, Journal of Materials Science: Materials in Electronics, **24**, 2426-2431, (2013).

[38] Özkurt, B., The mechanical properties of Y-doped Bi-2223 superconductors, Journal of Superconductivity and Novel Magnetism, **26**, 261-266, (2013).